crystals

MDPI

Article

Material and Technique Analysis of Qing Dynasty Official Style Architectural Polychrome Paintings in Hangzhou, Zhejiang, China

Ling Shen [1], Dan Hua [2], Baisu Nan [3], Yao Yao [3], Hong Duan [3] and Jiakun Wang [4,*]

[1] School of Art and Archaeology, Hangzhou City University, Hangzhou 310015, China; shenling@hzcu.edu.cn
[2] Xiaoshan District Museum, Hangzhou 311201, China
[3] Hangzhou Cultural Heritage and Historical Architecture Protection Center, Hangzhou 310002, China
[4] Guangdong Museum, Guangzhou 510623, China
* Correspondence: 17801230623@163.com

Abstract: Hangzhou was the political and economic center of the Southern Song Dynasty (1127–1279 AD) and also the southern end of the Beijing-Hangzhou Grand Canal during the Ming and Qing Dynasties (1368–1644 AD). This historical position allowed the city's economy to develop rapidly and influenced the form of its polychrome paintings with the imperial official style of the north China. However, due to the high temperature and rainy natural preservation conditions, southern polychrome paintings have always been a weak link in Chinese architectural polychrome painting craftsmanship. This study focuses on two well-preserved official-style architectural polychrome paintings in the grand halls from the late Qing period in Hangzhou. Through multi-techniques such as optical microscopy (OM), scanning electron microprobe with energy dispersive X-ray spectroscopy analysis (SEM-EDX), micro-Raman spectroscopy, micro-Fourier Transform Infrared spectroscopy (μ-FTIR), and pyrolysis-gas chromatography/mass spectrometry (Py-GC/MS), it was found that there is a significant difference from the reported common non-ground architectural paintings in the south, typically having four-layer structures with a white base and ground plaster layer in preparation for painting. The appearance of pigments such as artificial ultramarine ($Na_6Al_4Si_6S_4O_{20}$) and emerald green ($Cu(C_2H_3O_2)_2{\cdot}3Cu(AsO_2)_2$) indicates that the paintings were made at least after the 1830s, and the use of malachite green dye and copper phthalocyanine blue (PB 15:X) suggests that unrecorded restorations were also performed after the 20th century. All samples are coated with a layer of alkyd resin, which may have been added during the repairs in the latter half of the 20th century, leading to the black discoloration of the present paintings, especially in areas where emerald green was used. This study provides an important case for the study of the official style of polychrome painting craftsmanship in the southern region of China and also offers important references for the future protection and restoration of traditional architectural polychrome painting.

Keywords: architectural polychrome paintings; emerald green; organic coatings; multi-technique analysis

Academic Editor: Vladislav V. Gurzhiy

Received: 4 December 2024
Revised: 27 December 2024
Accepted: 31 December 2024
Published: 19 January 2025

Citation: Shen, L.; Hua, D.; Nan, B.; Yao, Y.; Duan, H.; Wang, J. Material and Technique Analysis of Qing Dynasty Official Style Architectural Polychrome Paintings in Hangzhou, Zhejiang, China. *Crystals* **2025**, *15*, 92. https://doi.org/10.3390/cryst15010092

1. Introduction

Polychrome paintings serve as the decorative elements of Chinese traditional architecture. They also constitute a significant part of wooden architectural structures, fulfilling functions such as fire prevention, moisture resistance, and decorative embellishment [1]. Different architectural painting techniques reflect the hierarchy of the buildings [2]. The

analysis of polychrome painting samples via scientific and technological methods holds substantial importance in exploring the original materials and production techniques employed in ancient times, as well as in determining the production era of pigments and their restoration history of the architectural paintings.

Due to the abundant extant cases and relatively continuous inheritance of the craftsmanship system for polychrome architectural paintings of the Qing Dynasty (1616–1911 AD), considerable research about official-style polychrome paintings has been attained [2–5]. Nevertheless, the majority of current studies are confined to the northern regions of China. In the Southeast area, due to the relatively high temperature and abundant rainfall, the preservation conditions for color paintings are unfavorable, and they are predominantly distributed among residential dwellings [6]. Presently, there is an urgent necessity to understand their materials and techniques, which will enable the comprehension of the differences in techniques between the northern and southern regions of China and facilitate the implementation of appropriate restoration in the future.

The objects of this investigation are the polychrome paintings on the main halls in Hangzhou during the late Qing Dynasty (1840–1912 AD). Hangzhou, the central area of Zhejiang Province in China, served as the political center during the Southern Song Dynasty (1127–1279 AD). Additionally, it is the southern terminus of the Beijing-Hangzhou Grand Canal, which has been listed as a UNESCO World Heritage Site. The Grand Canal in the Ming and Qing Dynasties promoted trade exchanges and cultural interactions between the north and the south of China. The two main halls under study are the Dacheng Hall (which means the great accomplishment) of the Confucius Temple and the Grand Hall of Qiyuan Buddhist Temple (Figure 1a). The Dacheng Hall is dedicated to the worship of the ancient sage Confucius and was constructed by official order. The Qiyuan Temple was an official temple during the Ming Dynasties (1386–1644 AD), yet the existing buildings were erected by private funds during the late Qing Dynasty. Owing to the presence of polychrome paintings in official temples, these two main halls represent relatively well-preserved examples in Hangzhou and constitute crucial cases for the research of color paintings in this region.

As can be observed from the interior hall photographs (Figure 1b,c), the architraves, and beams in the Dacheng Temple of Confucius Temple and the Grand Hall of Qiyuan Temple are filled with polychrome paintings. The ceilings (Figure 1b) of Dacheng Hall are decorated with impressive paintings. The compositions of the polychrome paintings in the two main halls are similar, with the main patterns on both ends of the beams and the rafters decorated with cloud and meander patterns. The main themes of the paintings are auspicious, including subjects such as dragons, phoenixes, Kylin, lions, cranes, landscapes, and stories of people. The similarities also can be discerned in the themes and dark and red color tones of the polychrome paintings. These similar patterns suggest that they might have been painted during a proximate period. In the early 20th century, certain analyses of the pigments were performed in Dacheng Hall of the Confucius Temple for maintenance. However, no explicit analysis data was retained. It was mentioned that the green pigment lacked the coloring element (Cu), and no further elaboration on the painting techniques was provided [7].

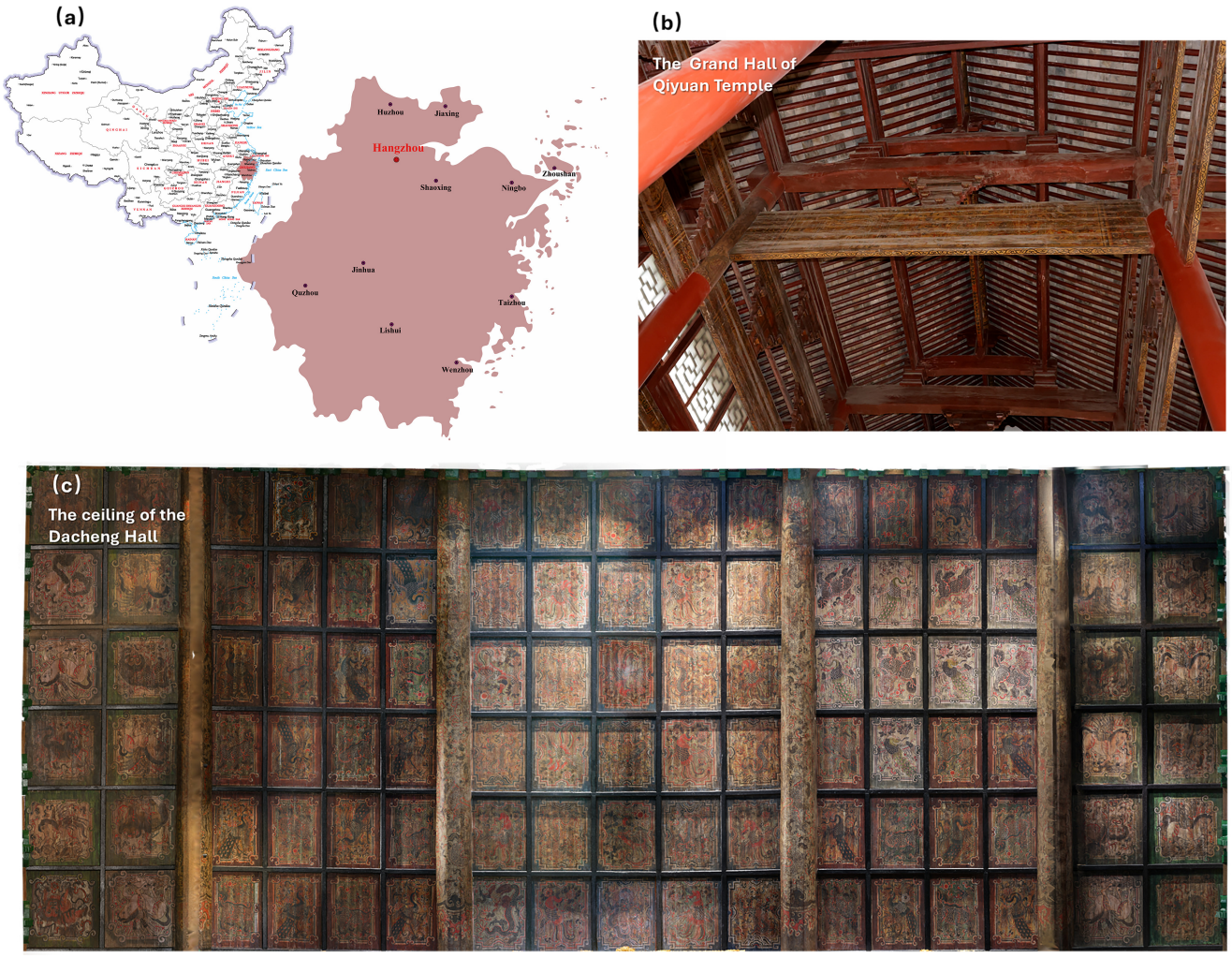

Figure 1. (**a**) A map of the location of Hangzhou. Images of the typical interior distribution of polychrome paintings on the (**b**) architraves in the Grand Hall of Qiyuan temple and (**c**) the ceilings of Dacheng Hall.

During the restoration works of the two main halls, we were fortuitous to obtain some representative samples, inimally invasive sampling was carried out. A variety of techniques were employed in the analysis of materials and processes.

Optical microscopic observation (OM), fluorescence microscopy (UV), and electron microscopy with energy dispersive X-ray spectroscopy (SEM-EDS) for morphological observation, and Raman spectroscopy for pigments identification in each layer were performed. Moreover, Micro-Attenuated Total Reflectance Fourier-Transform Infrared Spectroscopy (μ-ATR-FTIR) and pyrolysis gas chromatography-mass spectrometry (Py-GC/MS) were employed to further clarify the organic substances, thereby exploring the painting techniques of the hall color paintings in Hangzhou during the late Qing Dynasty.

2. Materials and Methods

2.1. The Object and Sampling Locations

In this study, samples collected from the Grand Hall in Qiyuan (QYS) Buddhist temple and the Hall of Dacheng (DCD) in the Confucius temple, with different color tones and different architectural components, were chosen for study, including many brownish parts (Figure 2) which the original colors cannot be recognized by eye. The information on the

sampling location and color is summarized in Table 1 and the optical images, including by visual light and UV light, of samples before embedding are illustrated in Figure 3.

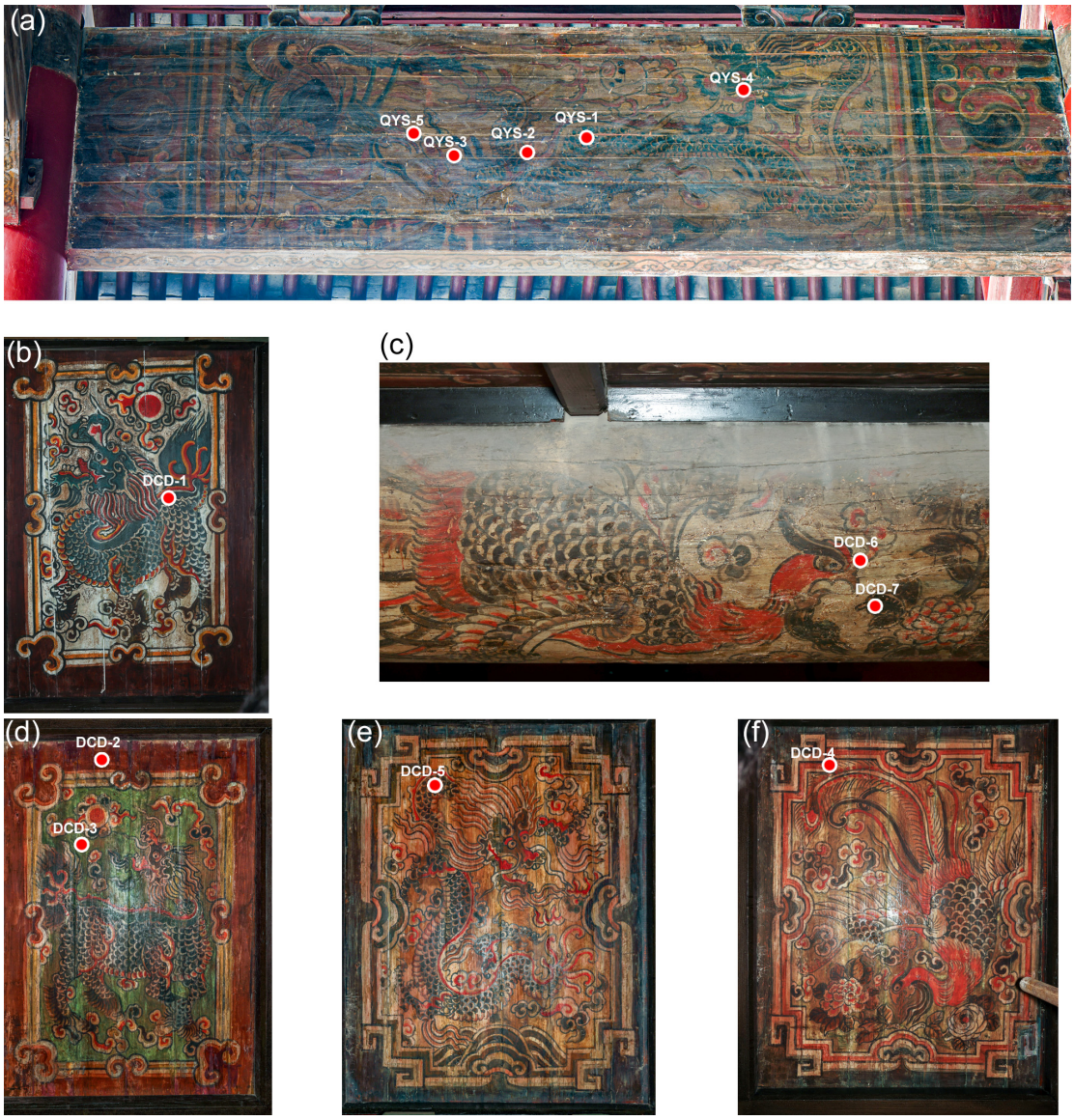

Figure 2. (**a**) The sampling locations on the architrave of the Grand Hall in Qiyuan temple; (**b**,**d**–**f**) the sampling locations on the ceiling of the Dacheng Hall; (**c**) the sampling locations on the beam of Dacheng Hall.

Table 1. Sampling location and appearance information of samples.

Location of the Samples	Positions in the Image	Samples Number	Visual Color Appearance of the Top Paint Layer
On the architrave in The Grand Hall of Qiyuan temple	The dragon scales	QYS-1	Green/blue
	The dorsal fin of the dragon	QYS-2	Red
	The dragon claw	QYS-3	Dark brown
	The dragon head	QYS-4	Green/blue
	The white base	QYS-5	White

Table 1. *Cont.*

Location of the Samples	Positions in the Image	Samples Number	Visual Color Appearance of the Top Paint Layer
On the ceiling of the Hall of Dacheng in Confucius Temple	The Kylin scales	DCD-1	Bright blue
	The edge of the Kylin image	DCD-2	Red
	The base ground color	DCD-3	Green
	The edge of the image	DCD-4	Red
	The dragon scales	DCD-5	Green
On the beam of the Hall of Dacheng in Confucius Temple	The head of the phoenix	DCD-6	Red
	The leaf	DCD-7	Dark brown

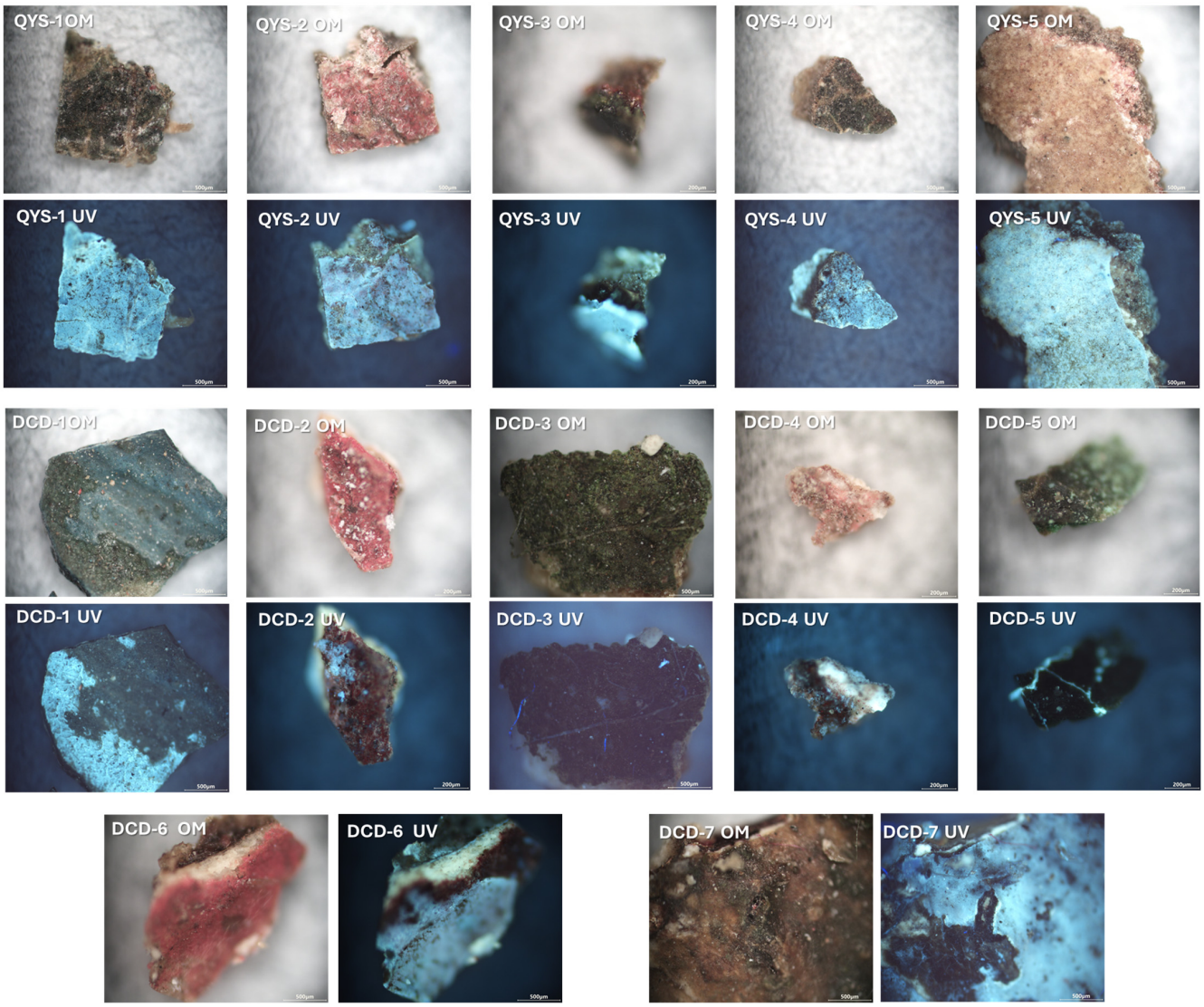

Figure 3. The optical microscopic images of samples under the visible light exposure (OM) and the ultraviolet (UV) light (365 nm).

2.2. Analytical Methods

2.2.1. Embedding

The basic characteristics of samples before and after embedding were observed with optical microscopy using a Sop-top RX 50M (Ningbo, China) microscope with 365 nm ultraviolet (UV) radiation light. The samples were embedded in cold inlay epoxy resin and dry polished with Micro-mesh® polishing cloths to the final step of 12000# mesh.

2.2.2. Micro-Raman Spectrometer

A micro-Raman spectroscope (DXR 2xi μ-Raman analyzer, New York, NY, USA) equipped with an EM-CCD detector was used. A 532 nm laser was used before embedding to qualitatively analyze the composition of the pigments. The Raman shift range was 100–3300 cm^{-1}; it took 2–10 s to acquire the data, performed 3–5 times with 0.1–2 mW power.

2.2.3. Scanning Electron Microscopy and Energy Dispersive X-Ray Spectroscopy (SEM-EDX)

Scanning electron microscopy (PhenomTM XL G2 SEM, Thermo Fisher Scientific, Eindhoven, The Netherlands) coupled with energy-dispersive X-ray spectroscopy (EDX) and a backscattering detector (BSE) was used to analyze the microstructure of the paint layers and semi-quantitatively analyze the major elements in the pigment minerals of different layers. Analysis was carried out in a low-vacuum environment (60 Pa), with a scanning voltage of 15 kV, and at a working distance of 7 mm.

2.2.4. Micro-Attenuated Total Reflectance Fourier-Transform Infrared Spectroscopy (μ-ATR-FTIR)

The cross-section exposed surface was analyzed by Thermo Scientific Nicolet iN10 Fourier-Transform Infrared Spectroscopy equipped with a microscope and the Thermo Scientific Nicolet iN10 Ge Tip ATR. The measured area ranges from 10 μm–10 μm × 50 μm–70 μm, scanning 64 times at a resolution of 4 cm^{-1}. The measuring wavenumber ranged from 680–4000 cm^{-1}. An OPUS 8.5 workstation was employed for IR analysis.

2.2.5. Pyrolysis-Gas Chromatography/Mass Spectrometry (Py-GC/MS)

Py-GC/MS analysis was conducted on an integrated system consisting of a pyrolyzer (Frontier EGA-PY3030D, Fukushima, Japan) and a gas chromatograph/mass spectrometer (Agilent 7890B/5977B, Santa Clara, CA, USA). The conditions used referred to the literature [8–10]. The GC system was equipped with an HP-5MS UI capillary column (30 m × 0.25 mm × 0.2 μm) with a quadrupole mass analyzer. The online methylated Py-GC/MS analysis included the following steps: less than 1 mg of sample, together with the methylation reagent (5 μL of 10 wt.% methanolic solution of tetramethylammonium hydroxide (TMAH, Aldrich, Shanghai, China)), was placed in the sample cup on top of the pyrolyzer at near-ambient temperature. Once the furnace temperature and GC/MS system were ready, the sample cup was introduced into the furnace and the temperature program of the GC oven was initiated. Pyrolysis was performed at 550 °C for 0.2 min. Helium was used as the carrier gas at a flow rate of 1.0 mL/min and with a split ratio of 10:1. The injector and GC/MS transfer line were maintained at 280 °C. The chromatographic conditions for the separation of the pyrolysis products included an initial temperature of 50 °C, which was then isothermal for 2 min, increased by 4 °C/min up to 280 °C, and then was isothermal again for 4 min. The MS detector operated at an ionizing voltage of 70 eV, the ion-source temperature was 230 °C, and the quadrupole temperature was 150 °C with a mass range m/z of 29–550. The NIST Library of Mass Spectra was used to identify the compounds.

3. Results

3.1. The Layered Structure with SEM-EDX and Raman Spectroscopy Analysis

As can be observed from Figure 3, the surfaces of the samples with red pigment exhibit a distinct and pronounced red color, while the blue-green shades are relatively dull (except for DCD-1). The sample DCD-5 is characterized by a black upper layer and a green lower layer. QYS-3, QYS-4, and DCD-7 display a dark brown color, with their original colors

being indistinguishable, possibly due to pigment discoloration that has resulted in the current palette being dominated by black and red on the polychrome painting.

Cross-sections were first examined with an optical microscope under visible and UV light to investigate the layer structure. Figure 4 presents QYS-3 and DCD-7 as representative samples. From the optical and ultraviolet photographs of the cross-sections, it can be observed that both exhibit similar stratigraphic structures. A transparent coating is present on the outermost layer, which emits a strong blue fluorescence under ultraviolet light. By integrating the elemental distribution characterizations obtained from electron microscopy, it is evident that the green sample layer contains copper (Cu) and arsenic (As), suggesting the possible presence of emerald green ($Cu(C_2H_3O_2)_2 \cdot 3Cu(AsO_2)_2$). The underlying white base layer is primarily composed of lead (Pb), which emits a yellow fluorescence under ultraviolet illumination, indicating the likely use of a lipid-based medium [11,12]. In the white base layer, QYS-3 only contains lead (Pb), while the white base layer of DCD-7 contains particles with some calcium (Ca) content. Beneath the white base layer, there is also a red layer; due to its thinness, it is currently unclear whether this layer contains lead-based red pigment or iron oxide red, and it is also unclear why this layer was painted above the ground layer. The most significant difference between the two halls lies in the ground layer: the samples from Qiyuan Temple's Daxiong Hall, beneath the white layer, are primarily composed of a ground plaster layer rich in silicon (Si), while the lower layer of Qiyuan Temple's Daxiong Hall is a white ground layer predominantly composed of calcium (Ca), likely calcite. Other samples from both halls also conform to this layer structure, and their optical photographs, UV images, and corresponding elemental distribution maps are presented in Figures S1 and S2.

The layer structures of samples DCD-1 and DCD-3 differ from the other samples. DCD-1 contains more complex multiple layers (Figure 5), especially with a thick blue pigment layer situated above a green pigment layer containing Cu and As, which suggests that the Kylin should have been a green one, followed by the white base layer, red layer, and ground plaster layer. The presence of a blue pigment layer indicates that the blue pigment may belong to a repainted layer. The element mapping shows that barium (Ba) and Zinc (Zn) are present in the blue pigment, suggesting the use of synthetic blue organic pigments mixed with lithopone (a mixture of baryte ($BaSO_4$) and ZnS), which were widely used in 1920s [13]. In contrast, the layer structure is shown in Figure 6. Directly beneath the Ba-containing green pigment layer of DCD-3 lies a calcium-rich ground layer, which reveals that green is used solely as a background base color for the ceiling portion of the image and green was painted directly onto the white ground layer.

To further elucidate the composition of the pigments, samples were subjected to Raman spectroscopy. The characteristic peaks from the Raman spectra, elemental analysis results, and the potential constituents are summarized in Table S1; the Raman spectra are illustrated in Figure S3 and the spectra of the green pigments are summarized in Figure 7. The samples in which this pigment was detected are listed in Table 2.

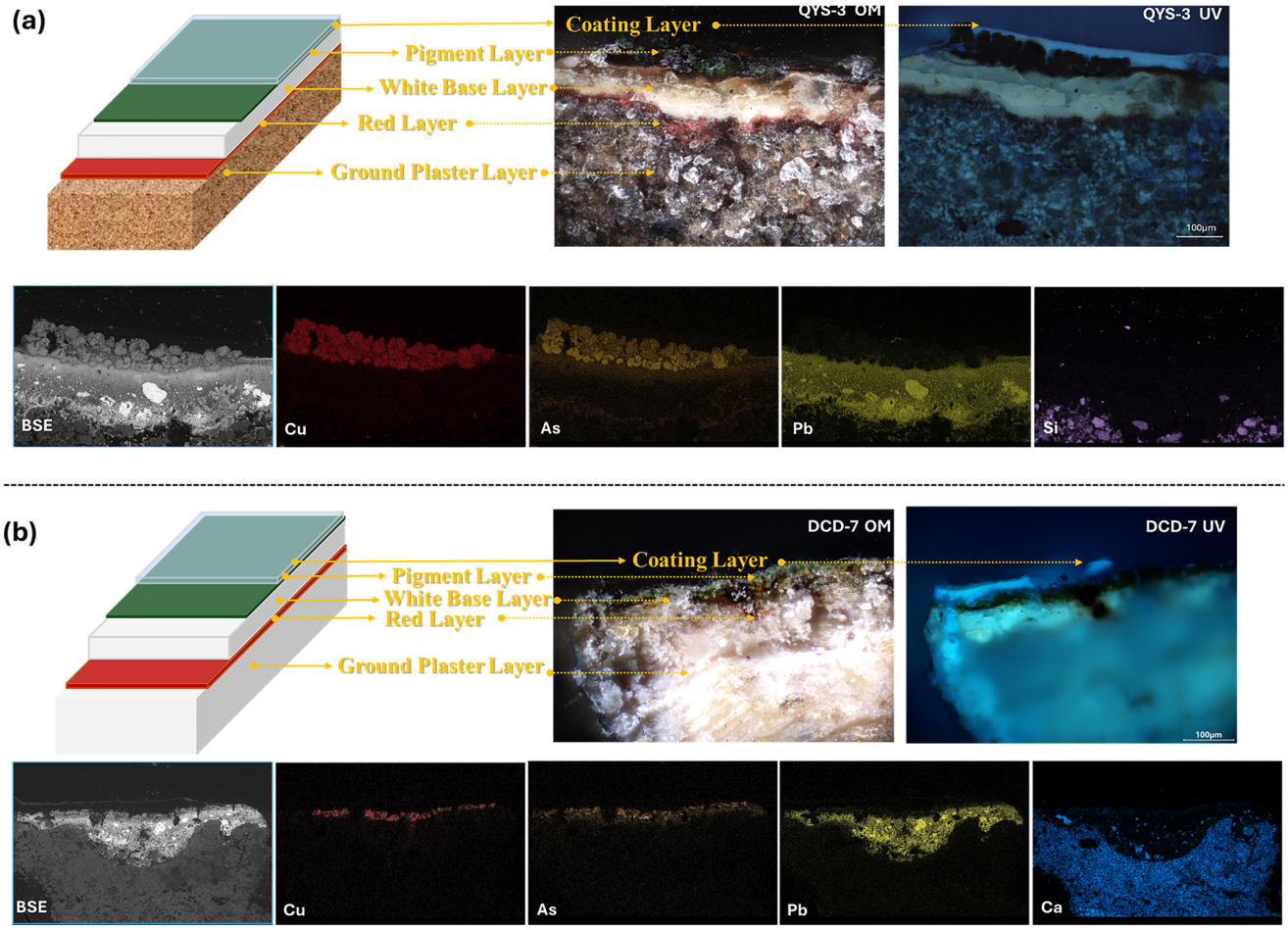

Figure 4. The representation of visible light optical images, UV images, and SEM-EDS elemental mapping results of samples of (**a**) QYS-3 with elements Cu, As, Pb, and Si and (**b**) DCD-7 with elements Cu, As, Pb, and Ca.

Table 2. The analysis results of the possible materials and the detected samples.

Layers	Possible Materials	Sampling No.
Pigment	Ultramarine	QYS-1
	Vermillion	QYS-2, DCD-2, DCD-4, DCD-6
	Emerald green	QYS-3, DCD-5, DCD-1,DCD-7
	Emerald green (original)	
	Prussian blue	QYS-4
	Blue: PB 15:X	DCD-1
	Malachite green	DCD-3
White base layer	Lead white	QYS-1, QYS-2, QYS-4, DCD-1, DCD-2, DCD-4, DCD-5, DCD-6, DCD-7
	Lead white (original)	QYS-3, DCD-1
Red layer	Hematite	QYS-1, QYS-3, QYS-4, DCD-1, DCD-2, DCD-4, DCD-6, DCD-7
Ground plaster layer	Calcite	DCD-1, DCD-2, DCD-3, DCD-4, DCD-6, DCD-7

Original: The pigments speculated to have been used originally based on the detected degenerated products.

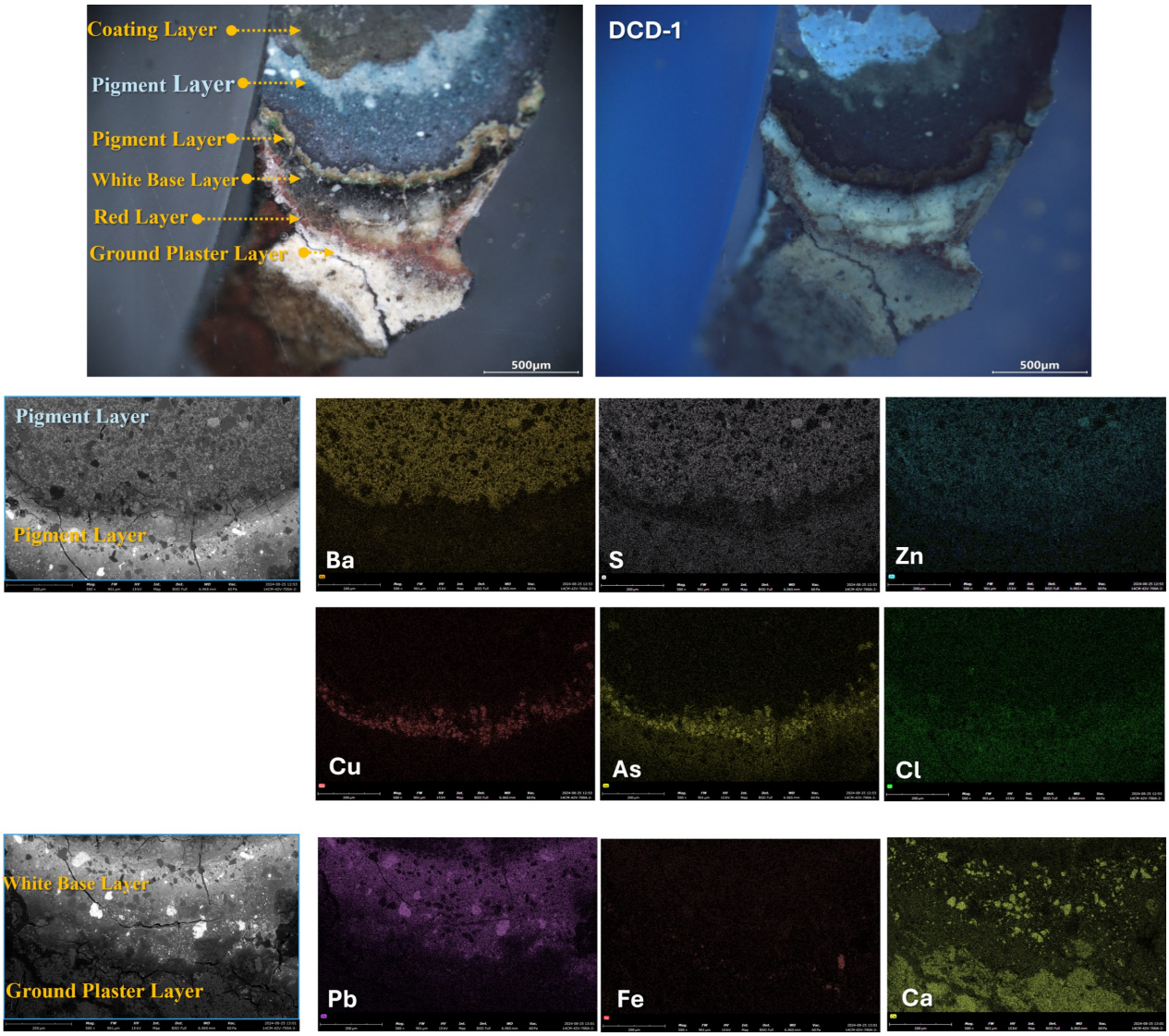

Figure 5. The visible light optical image and UV image of sample DCD-1 and the corresponding element distribution of Ba, S, Zn, Cu, As, and Cl in the pigment layer, and the elemental distribution of Pb, Fe, and Ca in the white base layer and ground layer.

The primary characteristic peaks in the red layer of samples have narrow peaks at r 220, 290 cm^{-1} and a strong peak at 1310 cm^{-1}, indicating that the layer predominantly consists of hematite (α-Fe_2O_3) [14]. The white base layers were uniformly subjected to lower energy levels (0.1 mW for testing) to prevent phase transformations induced by laser irradiation [15]. The Raman spectroscopy analysis results for the Qiyuan temple samples (QYS-1, QYS-3) illustrated the narrow band at 1050 cm^{-1}, which suggested, for the white base layer, that the peaks correspond to the characteristic strong peak of lead white (both hydrocerusite ($Pb(OH)_2 \cdot PbCO_3$) and cerussite ($PbCO_3$) could potentially be present) [16]. In the red layer of sample DCD-4, the characteristic bands of CO_3 symmetric stretching peaks are observed at 1085 cm^{-1}, indicating the presence of calcite ($CaCO_3$) within the white base layer, which also supports the results of EDS (Figure S2). In conjunction with the results indicating that mercury (Hg) was present in the surface red pigment layer, which were obtained from Energy-Dispersive X-ray Spectroscopy (EDS), Figure S3 shows that the band at 251 cm^{-1}, present in the spectra of red pigment in samples DCD-2, DCD-6, and QYS-2, further indicates that the red pigment predominantly employed in the surface layer is vermillion (HgS) [17]. According to the Raman spectroscopy results shown in Figure S3, it can be seen that the blue pigments include both ultramarine, with characteristic bands at

541 cm^{-1} and 1086 cm^{-1} (QYS-1), and Prussian blue ($Fe_4[Fe(CN)_6]_3$), with characteristic bands at 2148 cm^{-1} (QYS-4) [18,19].

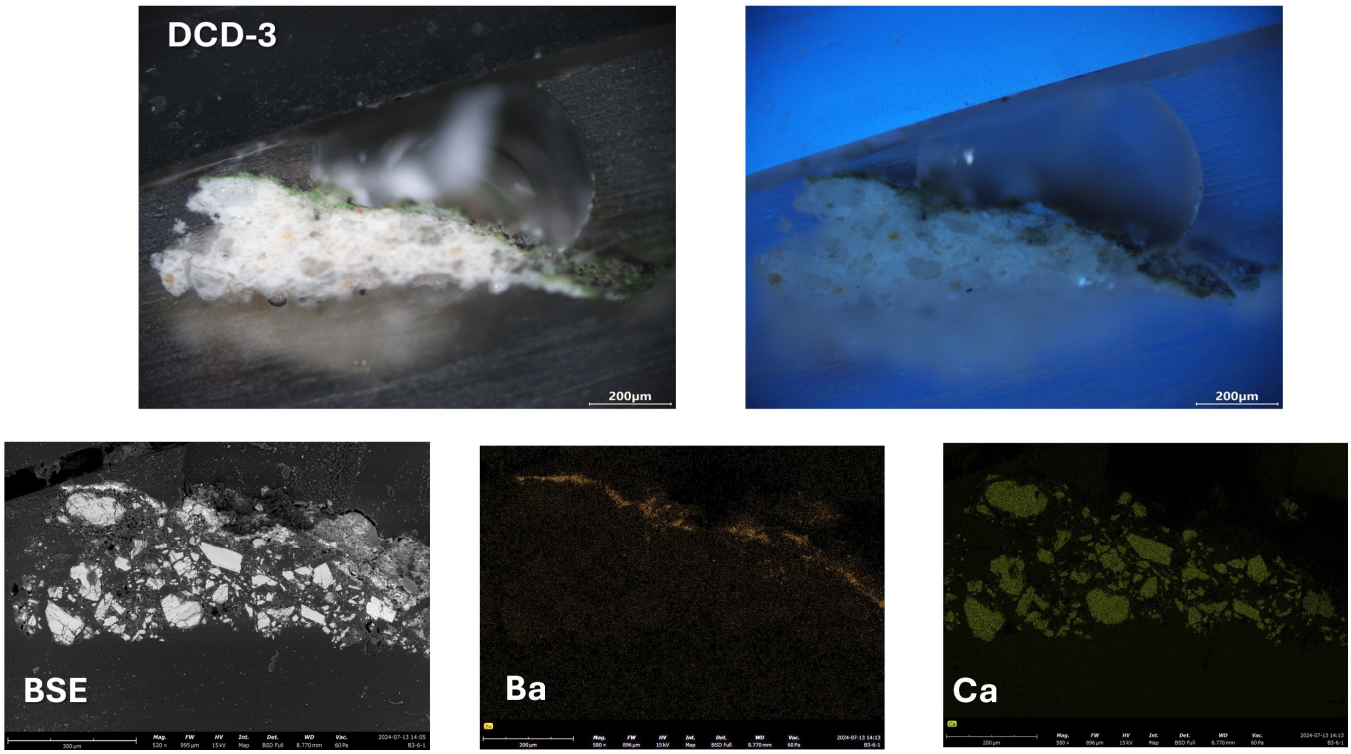

Figure 6. The visible light optical image and UV image of sample DCD-3 and the corresponding elemental distribution.

It is noteworthy that the green pigments appear black visually yet are discernible as green in cross-sections. This phenomenon can be observed in samples QYS-3, DCD-5, and DCD-7. EDS analysis indicates the presence of copper (Cu) and arsenic (As), suggesting that the pigment is likely to be emerald green. The Raman spectra of the green pigments in QYS-3 (Figure 7b) and DCD-5 show bands at 950 cm^{-1}, 490 and 217 cm^{-1}, which are the characteristic peaks that are consistent with emerald green [20–22]. Instead, in Figure 7a,c, the strongest band is at 830–850 cm^{-1}, which attributed to the vibration of AsO_4, indicating that in samples DCD-1 and DCD-7, the original emerald green pigments have undergone oxidation of As(III) to As(IV), and copper arsenates [23–25] are present. Emerald green with that characteristic peak at 830 cm^{-1} has also been reported in another case in southern Zhejiang, China [26]. Figure 8 illustrates the elemental distribution of green pigment particles in DCD-7. It can be observed from the figure that even within a single pigment particle, the elemental distribution is uneven. Cl and Ca are more concentrated in the surface layer. This suggests that Cl and Ca ions may have invaded from the surface and gradually reacted with emerald green.

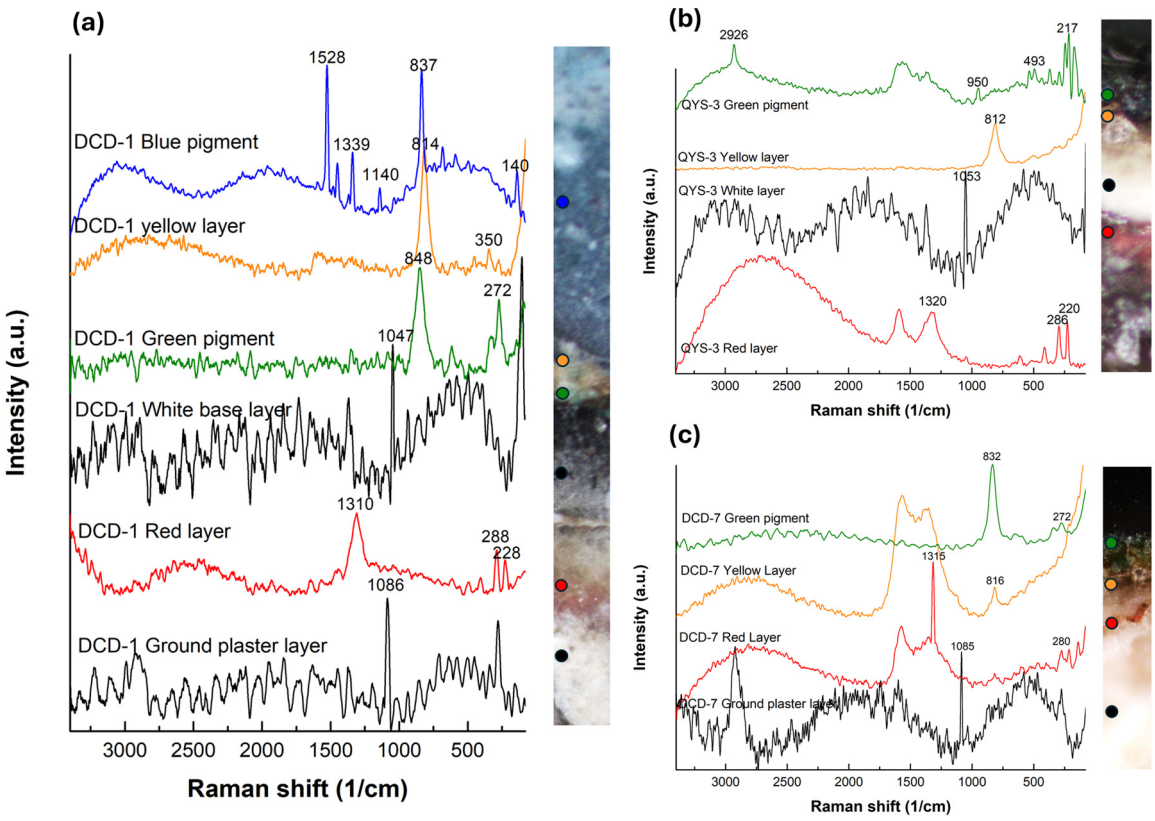

Figure 7. The Raman spectra of each layer for (**a**) sample DCD-1, (**b**) sample QYS-3, and (**c**) sample DCD-7.

Furthermore, the white base layer of the green samples has discolored and turned yellow. The peaks at 820 cm^{-1} suggest the possible presence of arsenate compounds [27–29]. The element mappings for the interface of green pigment and white base layer are illustrated in Figure S4. As ions migrated from the pigment particle, the Pb, As, and Cl distributed at the interface region. As is not only distributed within the green pigment layer but has also diffused and reacted with the surrounding lead white, resulting in the formation of lead arsenates such as mimetite ($Pb_5(AsO_4)_3Cl$). These degradation products between emerald green and lead white have also been reported in ref. [30].

In the samples from the Dacheng Hall, there is a special case, shown in Figure 2b, where DCD-1 was sampled from a painting with unique colors, and indeed, a more complex stratification is observed, suggesting that this ceiling painting may have been repainted. The characteristic strong peaks observed at 1528, 1340, and 1140 cm^{-1} of the bright blue areas are consistent with the characteristic peaks of copper phthalocyanine (PB-15:X) [31], which was first commercially marketed in 1935 [32]. Additionally, in DCD-3, there is an absence of a lead-containing white underlayer and red underlayer; the painting is directly executed on a calcium-containing ground layer. Furthermore, the Raman characteristic peaks of its green pigment are consistent with those of malachite green($C_{23}H_{25}N_2Cl$), a kind of synthetic triphenylmethane dye [33,34], which was discovered in Germany in the 19th century [35].

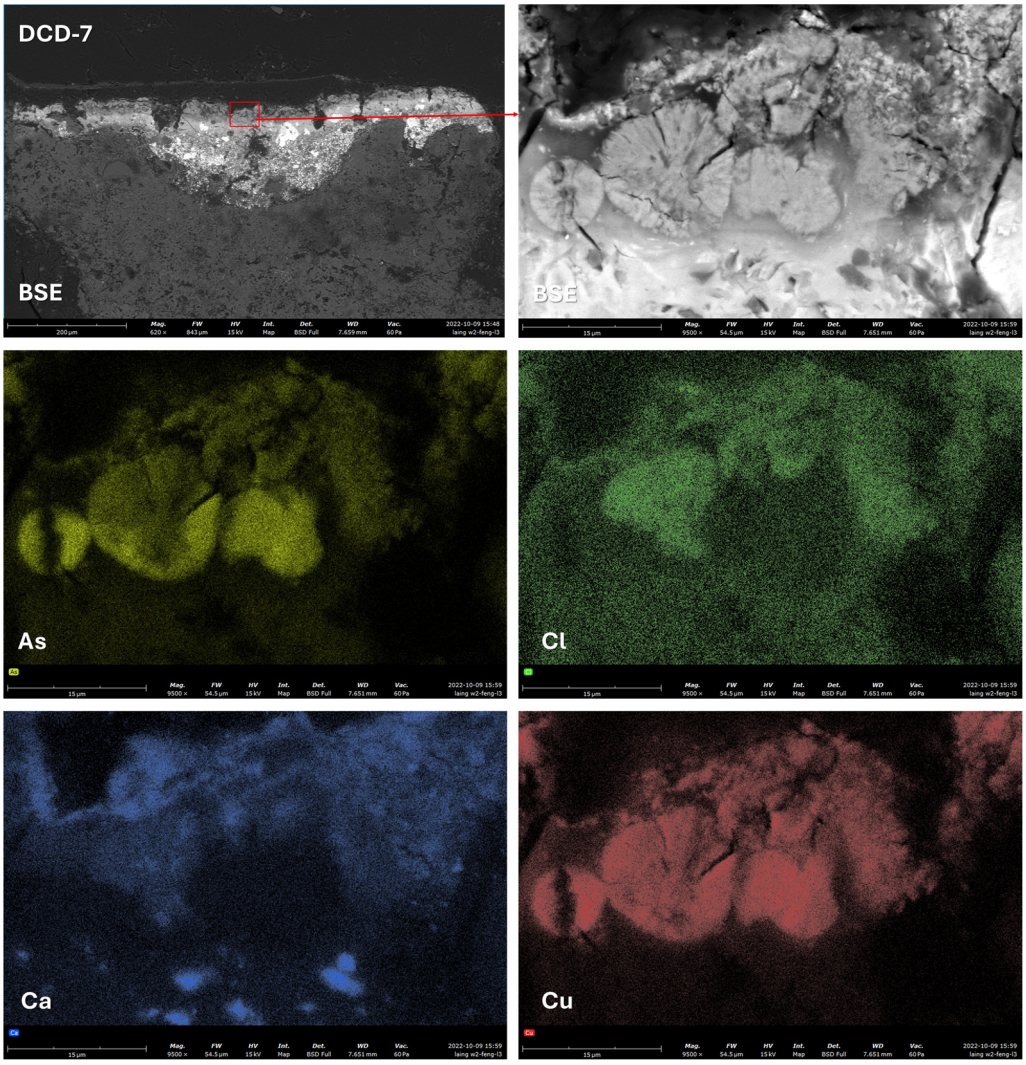

Figure 8. The element mapping of the green pigments in sample DCD-7 with elements Cu, As, Pb, and Cl.

3.2. Characterization of the Organic Materials

3.2.1. μ-ATR-FTIR

The use of μ-ATR-FTIR technology further clarifies the organic materials used in the samples, including the type of surface coating and the binder in the white base layer. The IR spectra of the surface coatings of various samples are shown in Figure 9a. Similar characteristic bands can be observed in these spectra, suggesting that the same kind of organic coating was applied. The bands at 1720, 1252, 1130, and 1070 cm^{-1} are consistent with alkyd resin [36]. The peaks at 1510, 1605, and 830 cm^{-1} observed in the spectra of DCD-7 and DCD-1 are due to the embedding epoxy resin (Figure S5). An unapparent peak at 1581 cm^{-1} could also be observed, which is probably due to the occurrence of copper carboxylates [37].

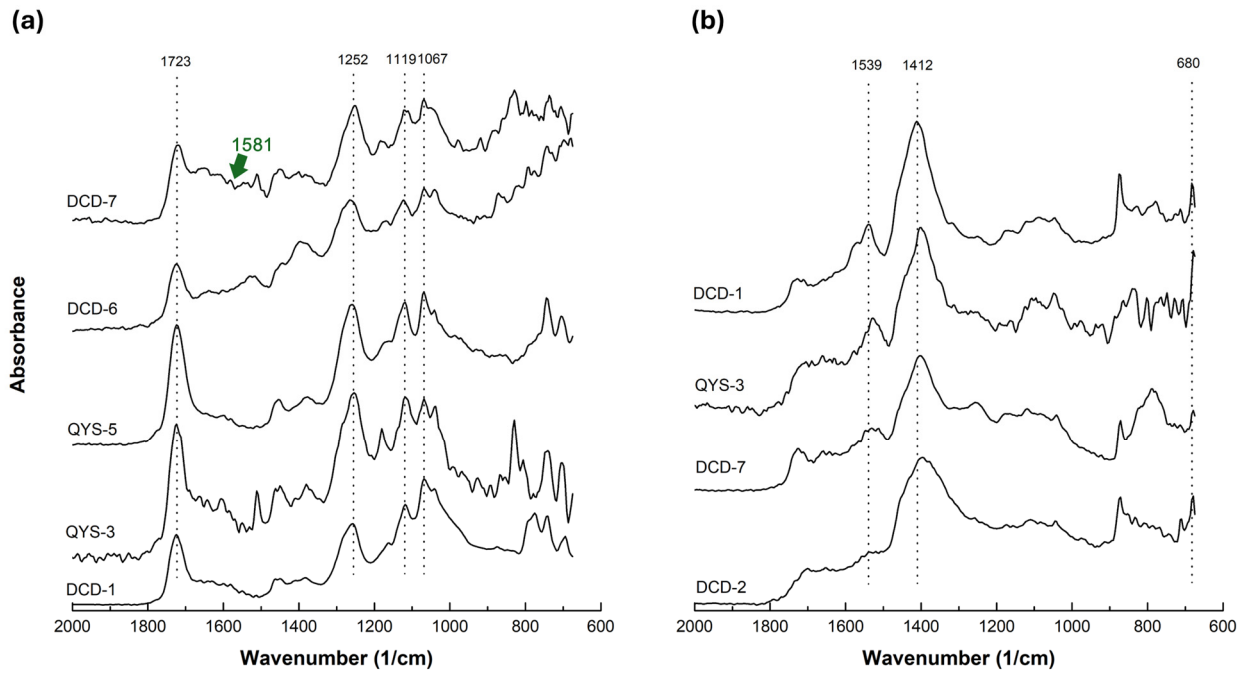

Figure 9. The ATR-FTIR spectra of (**a**) the surface coating layer and (**b**) the white base layer.

As for the white base layer IR spectra illustrated in Figure 9b, in QYS-3, only the characteristic peaks of lead white at 1404, 1045, and 680 cm^{-1} could be observed: 1404 cm^{-1} due to the antisymmetric C–O stretch of CO_3; 1045 cm^{-1} due to the symmetric C–O stretch of CO_3; and 680 cm^{-1} due to the C–O rocking deformation of CO_3 [38]. The characteristic band at 872 cm^{-1} for $CaCO_3$ was also present in the spectra of samples collected from Dacheng Hall (DCD-2, DCD-7, and DCD-1) [39], indicating that calcite was applied in the white layer within lead white. This also support the results of Raman spectroscopy and EDS analysis (Figures 5, 7, S2 and S3). The bands at 1539 cm^{-1} were due to the vibration of the anti-symmetric (COO−) stretch of lead carboxylates [40]. This also indicates that there may be grease present in this layer; however, the C=O vibrational peak around 1740 cm^{-1} overlaps with the C=O from the alkyd resin surface coating, thus making it impossible to ascertain the influence of the surface resin in that particular region.

3.2.1.1. Py-GC/MS

Samples DCD-7, QYS-3, DCD-4, and QYS-2 were selected as the typical samples and analyzed by pyrolysis-gas chromatography/mass spectrometry using thermally assisted hydrolysis and methylation (THM-Py-GC/MS), which is an efficient and accurate way to identify the drying oil in artifacts [41–43]. A series of monocarboxylic and dicarboxylic acids were detected and are illustrated in Figure 10, as well as the pyrolysis products listed in Table S1, indicate that drying oils were added to the polychrome painting. The phthalic compounds dimethyl phthalate (RT. at 25.607 min) and benzoic acid (RT. at 13.073 min) may be present due to the surface coating [44]. The markers of lacquer (methyl/dimethyl esters of phenol [43]) were detected, indicating that raw lacquer was not applied during the priming process. The TICs of other samples are illustrated in Figure S5, and the important compounds obtained in these polychrome painting samples are listed in Tables S3–S5. TICs indicate that the main substances are identical. A/P and P/S values are used to identify the type of drying oil. In Table 3, the ratios based on the area of TIC of palmitic acid to stearic acid (P/S) and azelaic acid to palmitic acid (A/P) ranged from 1.29 to 1.64 and from 0.67 to 1.67, respectively, indicating the presence of raw tung oil or linseed oil and walnut oil in

the samples [41]. However, there is significant value variation among the samples, which may be attributed to factors such as the type of pigment and the aging time.

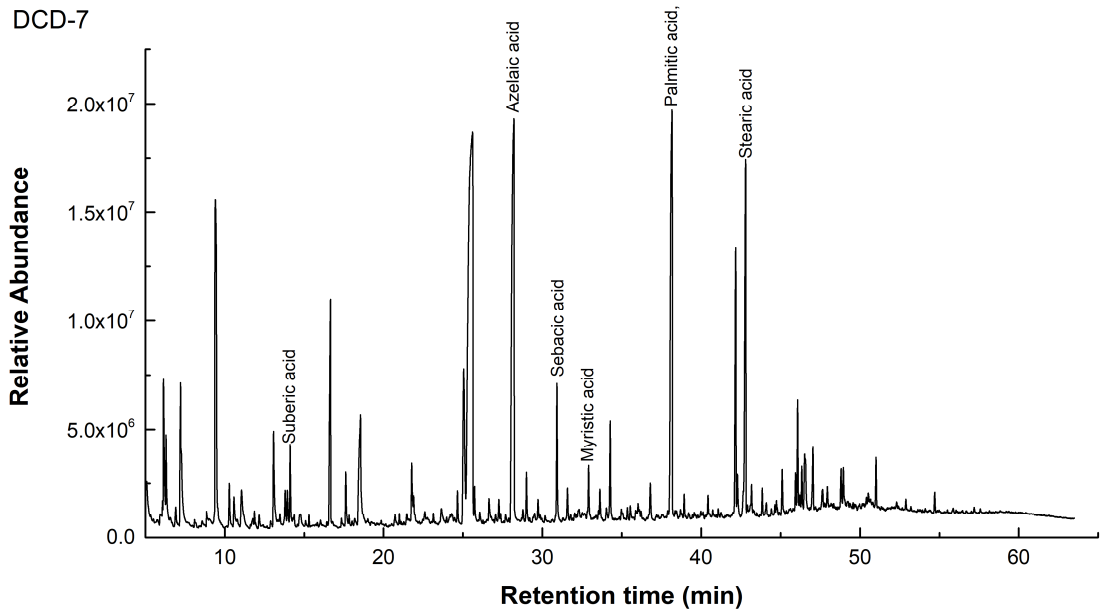

Figure 10. The total ion chromatogram (TIC) of sample DCD-7.

Table 3. The P/S and A/P values of different samples.

Sample	A/P	P/S
DCD-7	1.32	1.64
QYS-3	1.67	1.29
DCD-4	0.93	1.99
QYS-2	0.67	1.50

4. Discussion

The Prussian blue, synthetic ultramarine, vermillion, and emerald green used in the two polychrome paintings are common pigments found in the colored paintings of the late Qing Dynasty [20]. However, DCD-1 utilized pigment PB 15:X, which began to commercially circulate after the 1930s. The simultaneous use of alkyd resin as a protective material in both main halls suggests that they were likely restored at the same time, which, according to the restoration records of Qiyuan Temple, probably occurred in the 1980s. This indicates that the Dacheng Hall underwent repainting of the Kylin ceiling mural between 1940 and 1980.

Although many areas appear black in the polychrome painting, the findings of this study suggest that these areas use green pigments, specifically emerald green. This finding would significantly alter the understanding of color palettes in Hangzhou and the southern regions. Despite the green surfaces turning brown over time, there was no significant spectral difference observed in Figure 9b. The peak for copper fatty acids at 1580 cm^{-1} was not particularly pronounced, possibly due to the limited crystalline regions and the relatively large measured area (20 μm). Additionally, peaks at 1580 cm^{-1} are influenced by the vibrational bands due to the aromatic stretching of alkyd resin [45], thus necessitating further investigation into the spectral influence of this region using microscopic representation methods. To date, there have been no reports on the relationship between modern restoration materials and pigment aging. If alkyd resins were widely used during that

time, further research into the reaction mechanisms of Cu and As ions would be required to provide a scientific basis for subsequent coating selection.

Furthermore, this study diverges from previous research in the southern regions of China, which currently posits that the south predominantly lacks a ground layer, using raw lacquer as the base color with a white layer and pigment layer applied on top [46,47]. However, this study has uncovered a new approach for preparing architectural polychrome painting: the absence of detectable lacquer substances suggests that a leveling layer, likely a mixture of oil with earthern plaster/calcite, was used on the wooden substrate, followed by an application of oil and lead white. The middle red layer may constitute the base color. Due to the thinness of the red layer, its organic binder remains undetermined. Moreover, the surface alkyd resin significantly affects infrared detection, and it is currently impossible to accurately determine the types of organic compounds in each layer using spectral techniques.

5. Conclusions

This study analyzed the materials used in the architectural polychrome paintings in Hangzhou, Zhejiang, China. We selected two main halls as representatives and collected samples of various components and colors from them. Through cross-sectional observation, it was found that these two halls have very similar structures: a ground plaster layer—red pigment layer—white base layer—pigment layer—surface coating. However, the materials of the ground plaster layer are different, with earthen materials applied in the Grand Hall of Qiyuan temple and a white lime layer used in Dacheng Hall. This four-layer structure is the first to be discovered in the polychrome paintings of southern China, differing from the situation mainly dominated by non-ground polychrome paintings introduced in previous articles. This enriches the understanding of southern polychrome paintings and provides further evidence for the study of traditional crafts.

In addition, this study found that the colors of the polychrome paintings are richer than the red and black tones observed by the naked eye. Blue was used in the form of artificial ultramarine and Prussian blue, indicating that different blue tones were likely created. Moreover, many brown-black areas, such as dragon claws, dragon fins, phoenix feathers, and plants, in the patterns were likely green but have discolored due to the influence of restoration materials. This study did not adequately explain this phenomenon from the perspective of products and reaction mechanisms. However, this issue may be widespread in southern China region, making it worthwhile to delve into the study of pigment discoloration and crystallization issues with different restoration materials.

Supplementary Materials: The following supporting information can be downloaded at: https://www.mdpi.com/article/10.3390/cryst15010092/s1, Figure S1. The visible light optical image, UV image, and the corresponding element distribution for sample QYS-1, sample QYS-2, sample QYS-4, and sample QYS-5. Figure S2. The visible light optical image, UV image, and the corresponding element distribution for sample DCD-2, sample DCD-4, sample DCD-5, and sample DCD-7. Figure S3. The Raman spectra of sample QYS-1, sample QYS-2, sample QYS-4, sample DCD-2, sample DCD-3, sample DCD-4, sample DCD-5, and sample DCD-6. Table S1. The analysis results of EDS and Raman spectroscopy for each layer and the possible materials. Figure S4. The corresponding element distribution for sample DCD-1, sample QYS-3, and sample DCD-7. Figure S5. The IR spectrum of the embedding resin. Table S2. The pyrolysis products of DCD-7. Figure S6. The TICs of samples QYS-3, DCD-4, and QYS-2. Table S3. The pyrolysis products of QYS-3. Table S4. The pyrolysis products of DCD-4. Table S5. The pyrolysis products of QYS-2.

Author Contributions: Conceptualization, L.S. and J.W.; methodology, L.S.; software, J.W.; validation, B.N., Y.Y. and H.D.; formal analysis, D.H.; investigation, J.W.; resources, D.H. and B.N.; data curation, L.S.; writing—original draft preparation, L.S.; writing—review and editing, J.W.; visualization, L.S.;

supervision, L.S.; project administration, L.S.; funding acquisition, L.S. All authors have read and agreed to the published version of the manuscript.

Funding: This research was funded by Conservation Science and Technology Project of Zhejiang Provincial Administration of Cultural Heritage (grant number 2023014) an Hangzhou Philosophy and Social Science Planning Project (grant number Z23JC099).

Data Availability Statement: The data presented in this study are available on request from the corresponding author.

Acknowledgments: Thank you to the Zhejiang Provincial Bureau of Cultural Relics for providing the opportunity and financial support for this research.

Conflicts of Interest: The authors declare no conflicts of interest.

References

1. Liu, L.Y.; Zhang, B.J.; Yang, H.; Zhang, Q. The Analysis of the Colored Paintings from the Yanxi Hall in the Forbidden City. *Spectrosc. Spectr. Anal.* **2018**, *38*, 2054–2063.
2. Zhuo, Y.Y.; Wang, S.J. On the Construction History and Craftsmanship of the Polychrome Patterns on the Inner Eaves of the Rear Hall of Fengxian Dian in the Forbidden City. *Palace Mus. J.* **2024**, *10*, 35–55+147.
3. Jiang, G.Q. *Official Architectural Color Painting Techniques of the Qing Dynasty in China*; China Architecture & Building Press: Beijing, China, 2005.
4. Liu, M.Y. *Research on Pigments for Decorative Polychrome Painting in Official Handicraft Regulations and Precedents of the Qing Dynasty*; Tsinghua University: Beijing, China, 2019.
5. Li, Y.; Liu, M.Y. A Study of The Materials and Techniques Used in The Polychrome Ceiling Decoration of The Linxi Pavilion in The Garden of The Cining Palace. *Palace Mus. J.* **2018**, *6*, 45–63.
6. Gong, D.C.; Hu, S.; He, W.J. *Research on the Conservation Techniques and Traditional Crafts of Jiangnan Ancient Architectural Polychrome Paintings*; Cultural Relics Press: Beijing, China, 2013.
7. Du, Z.X. *Hangzhou Confucius Temple Polychrome Paintings*; Zhejiang People's Publishing House: Hangzhou, China, 2008.
8. Shen, L.; Kang, Y.; Li, Q. Analytical Study of Polychrome Clay Sculptures in the Five-Dragon Taoist Palace of Wudang, China. *Coatings* **2024**, *14*, 540. [CrossRef]
9. Zhou, Z.; Shen, L.; Li, C.; Wang, N.; Chen, X.; Yang, J.; Zhang, H. Investigation of gilding materials and techniques in wall paintings of Kizil Grottoes. *Microchem. J.* **2020**, *154*, 104548. [CrossRef]
10. Yang, J.; Zhou, Z.; Lu, T.; Shen, L. Investigation of Gold Gilding Materials and Techniques Applied in the Murals of Kizil Grottoes, Xinjiang, China. *Appl. Sci.* **2022**, *12*, 11202. [CrossRef]
11. Sandu, I.C.A.; Schäfer, S.; Magrini, D.; Bracci, S.; Roque, C.A. Cross-Section and Staining-Based Techniques for Investigating Organic Materials in Painted and Polychrome Works of Art: A Review. *Microsc. Microanal.* **2012**, *18*, 860–875. [CrossRef]
12. Platania, E.; Streeton, N.L.W.; Lluveras-Tenorio, A.; Vila, A.; Buti, D.; Caruso, F.; Kutzke, H.; Karlsson, A.; Colombini, M.P.; Uggerud, E. Identification of green pigments and binders in late medieval painted wings from Norwegian churches. *Microchem. J.* **2020**, *156*, 104811. [CrossRef]
13. Feller, R.L. *Artists' Pigments a Handbook of Their History and Characteristics Volume 1*; Archetype Publications: London, UK, 2012.
14. Froment, F.; Tournié, A.; Colomban, P. Raman identification of natural red to yellow pigments: Ochre and iron-containing ores. *J. Raman Spectrosc.* **2008**, *39*, 560–568. [CrossRef]
15. Costantini, I.; Lottici, P.P.; Castro, K.; Madariaga, J.M. Use of Temperature Controlled Stage Confocal Raman Microscopy to Study Phase Transition of Lead Dioxide (Plattnerite). *Minerals* **2020**, *10*, 468. [CrossRef]
16. Search RRUFF Sample Data. Available online: https://rruff.info/ (accessed on 31 December 2024).
17. Burgio, L.; Clark, R.J. Library of FT-Raman spectra of pigments, minerals, pigment media and varnishes, and supplement to existing library of Raman spectra of pigments with visible excitation. *Spectrochim. Acta A Mol. Biomol. Spectrosc.* **2001**, *57*, 1491–1521. [CrossRef] [PubMed]
18. Bell, I.M.; Clark, R.J.H.; Gibbs, P.J. Raman spectroscopic library of natural and synthetic pigments (pre-1850AD). *Spectrochim. Acta A* **1997**, *53*, 2159–2179. [CrossRef]
19. Rosi, F.; Miliani, C.; Borgia, I.; Brunetti, B.; Sgamellotti, A. Identification of nineteenth century blue and green pigments by in situ x-ray fluorescence and micro-Raman spectroscopy. *J. Raman Spectrosc.* **2004**, *35*, 610–615. [CrossRef]
20. Zheng, Y.; He, X.; Li, X.; Chen, K.; Guo, H.; Pan, X. Raman Spectroscopy Analysis of the Mural Pigments in Lam Rim Hall of Wudang Lamasery, Baotou Area, Inner Mongolia, China. *Minerals* **2022**, *12*, 456. [CrossRef]

21. Herm, C. Emerald Green versus Scheele's Green: Evidence and Occurrence. In Proceedings of the 7th Interdisciplinary ALMA Conference, Bratislava, Slovak, 16–18 October 2019.
22. Petrova, O.; Pankin, D.; Povolotckaia, A.; Borisov, E.; Krivul Ko, T.; Kurganov, N.; Kurochkin, A. Pigment palette study of the XIX century plafond painting by Raman spectroscopy. *J. Cult. Herit.* **2019**, *37*, 233–237. [CrossRef]
23. Sun, F.; Wang, R.S.; Qi, D.S.; Yan, H.H. Degradation of emerald green pigment in painted grottoes in Sichuan, China. *J. Cult. Herit.* **2024**, *69*, 1–9. [CrossRef]
24. Frost, R.L.; Martens, W.N.; Williams, P.A. Raman spectroscopy of the phase-related basic copper arsenate minerals olivenite, cornwallite, cornubite and clinoclase. *J. Raman Spectrosc.* **2002**, *33*, 475–484. [CrossRef]
25. Martens, W.N.; Frost, R.L.; Kloprogge, J.T.; Williams, P.A. The basic copper arsenate minerals olivenite, cornubite, cornwallite and clinoclase: An infrared emission and Raman spectroscopic study. *Am. Mineral.* **2003**, *88*, 501–508. [CrossRef]
26. Shen, L.; Wang, C.; Zhang, J.; Cui, B.; Zhu, S.; Mao, J. Cu and As containing pigments in Zhejiang architecture polychrome paintings: A case study of degradation products of emerald green. *Herit. Sci.* **2023**, *11*, 9–14. [CrossRef]
27. Bajda, T. Solubility of mimetite $Pb_5(AsO_4)_3Cl$ at 5–55 °C. *Environ. Chem.* **2010**, *7*, 268. [CrossRef]
28. Frost, R.L.; Bouzaid, J.M.; Palmer, S. The structure of mimetite, arsenian pyromorphite and hedyphane—A Raman spectroscopic study. *Polyhedron* **2007**, *26*, 2964–2970. [CrossRef]
29. Liu, Z.; Xu, W.; Zhang, Y.; Wang, Y.; Li, J. Identification of the Pigments on the Mural Paintings from an Ancient Chinese Tomb of Tang Dynasty Using Micro-Raman and Scanning Electron Microscopy/Energy Dispersive X-ray Spectroscopy Analysis. *Minerals* **2023**, *13*, 1224. [CrossRef]
30. Li, Z.; Wang, L.; Chen, H.; Ma, Q. Degradation of emerald green: Scientific studies on multi-polychrome Vairocana Statue in Dazu Rock Carvings, Chongqing, China. *Herit. Sci.* **2020**, *8*, 64. [CrossRef]
31. Marcelino, M.D.R.; Muralha, V.S.F. Synthetic organic pigments in contemporary Balinese painting: A Raman microscopy study. *J. Raman Spectrosc.* **2012**, *43*, 1281–1292. [CrossRef]
32. Lomax, S.Q.; Lomax, J.F.; Luca-Westrate, A.D. The use of Raman microscopy and laser desorption ionization mass spectrometry in the examination of synthetic organic pigments in modern works of art. *J. Raman Spectrosc.* **2014**, *45*, 448–455. [CrossRef]
33. Liu, J.; Zha, D.; Chen, X.; Wang, Y.; Wang, Z.; Li, Z. Comparison of malachite green adsorption by two yeast strains using Raman microspectroscopy. *FEMS Microbiol. Lett.* **2019**, *366*, fnz163. [CrossRef]
34. Zhang, Y.; Yu, W.; Pei, L.; Lai, K.; Rasco, B.A.; Huang, Y. Rapid analysis of malachite green and leucomalachite green in fish muscles with surface-enhanced resonance Raman scattering. *Food Chem.* **2015**, *169*, 80–84. [CrossRef]
35. Cooksey, C. Quirks of Dye Nomenclature. 6. Malachite Green. *Biotech. Histochem.* **2016**, *91*, 438–444. [CrossRef]
36. Ploeger, R.; Scalarone, D.; Chiantore, O. The characterization of commercial artists' alkyd paints. *J. Cult. Herit.* **2008**, *9*, 412–419. [CrossRef]
37. Izzo, F.C.; Kratter, M.; Nevin, A.; Zendri, E. Critical Review on the Analysis of Metal Soaps in Oil Paintings. *ChemistryOpen* **2021**, *10*, 904–921. [CrossRef]
38. Goltz, D.; Mcclelland, J.; Schellenberg, A.; Attas, M.; Cloutis, E.; Collins, C. Spectroscopic studies on the darkening of lead white. *Appl. Spectrosc.* **2003**, *57*, 1393–1398. [CrossRef] [PubMed]
39. Myszka, B.; Schussler, M.; Hurle, K.; Demmert, B.; Detsch, R.; Boccaccini, A.R.; Wolf, S.E. Phase-specific bioactivity and altered Ostwald ripening pathways of calcium carbonate polymorphs in simulated body fluid. *RSC Adv.* **2019**, *9*, 18232–18244. [CrossRef] [PubMed]
40. Liu, G.; Guerreiro, E.; Babington, C.; Kazarian, S.G. ATR-FTIR spectroscopic imaging of white crusts in cross sections from oil cartoons by Edward Poynter in the Heritage Collections at UK Parliament. *J. Cult. Herit.* **2023**, *62*, 251–267. [CrossRef]
41. Wang, N.; He, L.; Zhao, X.; Simon, S. Comparative analysis of eastern and western drying-oil binding media used in polychromic artworks by pyrolysis-gas chromatography/mass spectrometry under the influence of pigments. *Microchem. J.* **2015**, *123*, 201–210. [CrossRef]
42. Wang, X.; Zhen, G.; Hao, X.; Zhou, P.; Wang, Z.; Jia, J.; Gao, Y.; Dong, S.; Tong, H. Micro-Raman, XRD and THM-Py-GC/MS analysis to characterize the materials used in the Eleven-Faced Guanyin of the Du Le Temple of the Liao Dynasty, China. *Microchem. J.* **2021**, *171*, 106828. [CrossRef]
43. Hao, X.; Schilling, M.R.; Wang, X.; Khanjian, H.; Heginbotham, A.; Han, J.; Auffret, S.; Wu, X. Use of THM-PY-GC/MS technique to characterize complex, multilayered Chinese lacquer. *J. Anal. Appl. Pyrol.* **2019**, *140*, 339–348. [CrossRef]
44. Wei, S.; Pintus, V.; Schreiner, M. A comparison study of alkyd resin used in art works by Py-GC/MS and GC/MS: The influence of aging. *J. Anal. Appl. Pyrol.* **2013**, *104*, 441–447. [CrossRef]
45. Kappler, A.; Fischer, M.; Scholz-Bottcher, B.M.; Oberbeckmann, S.; Labrenz, M.; Fischer, D.; Eichhorn, K.J.; Voit, B. Comparison of mu-ATR-FTIR spectroscopy and py-GCMS as identification tools for microplastic particles and fibers isolated from river sediments. *Anal. Bioanal. Chem.* **2018**, *410*, 5313–5327. [CrossRef]

46. He, W.J. Traditional Technique of Colored Paintings on Unplastered Wooden Surface of Ancient Architectures in Jiangsu. *Southeast Cult.* **2009**, *5*, 101–107.
47. He, W.J.; Yang, X.Q.; Jiang, F.R.; Gong, D.C.; Zheng, D.Q.; Zhang, Z.M.; Wang, M.J. Study on the conservation of colored paintings on unplastered wooden surface used in Zhao Yongxian's mansion of Changshu. *Sci. Conserv. Archaeol.* **2008**, *20*, 55–60.